Spatiotemporal Stochastic Resonance in Excitable Media

Peter Jung and Gottfried Mayer-Kress
Department of Physics and Center of Complex Systems Research, Beckman Institute, University of Illinois at Urbana-Champaign, Urbana, Illinois 61801
(Received 20 September 1994)

We present first numerical evidence that in an excitable medium the synchronization of spatiotemporal patterns with external excitatory waves shows a sharp peak at a finite, well-defined noise level independent of the system size. This effect can be understood as a generalization of the concept of stochastic resonance to spatially extended systems. We further show the impact of spatiotemporal stochastic resonance for the spreading of spiral waves, where the noise level controls the scale and size of the spiral.

PACS numbers: 82.40.–g, 05.40.+j, 47.54.+r

Pattern formation far from equilibrium has been studied very extensively in the last years (for a recent review, see [1,2]). Representative examples are Rayleigh-Bénard convection rolls, Taylor-Couette flow, and spiral waves in the Belousov-Zhabotinsky reaction. Typically a pattern starts to build up when the control parameter (the temperature difference in case of the Rayleigh-Bénard system) becomes larger than a critical value. Noise makes the bifurcation smooth by triggering the onset of the pattern even below threshold $r < r_c$. The role of fluctuations for the onset and selection of patterns has been studied in some detail and is reported on in a number of articles in [3,4] and [5]. In this paper, we discuss the role of noise for the formation of patterns in two-dimensional excitable media from a different perspective.

It has been shown that a certain amount of noise can amplify temporal patterns by increasing the system's sensitivity via stochastic resonance [6] (for recent reviews, see [7,8]). This effect has been shown first for symmetric bistable systems. The external forcing (the temporal pattern) tilts the bistable potential weakly back and force (weak enough that the potential remains bistable), thereby modulating the barrier height for noise-induced hopping between the stable domains. The synchronization of the hopping with the external forcing shows a bell-shaped curve as a function of the noise strength—the fingerprint of stochastic resonance. Only recently, stochastic resonance has been demonstrated in much simpler systems, namely in threshold devices [9–11]. Here, Gaussian noise and a periodic signal is applied to a threshold device which responds with a spike if the sum of the noise and the signal is crossing the threshold from below. The intensity of the peak at the signal frequency in the power spectrum of the outgoing spike train shows a bell-shaped curve as a function of the variance of the noise. At the maximum, the variance of the noise matches half the square of the threshold—a result which we will make heavy use of in this paper. The basic question we study in this paper is in how far stochastic resonance can also be observed in spatially extended pattern forming systems.

As a working model, we use a two-dimensional equidistant square array (lattice constant a) of $N \times N$ noisy threshold devices [9] $d_{ij} : x_{ij}(t) \rightarrow s_{ij}(t)$ ($i = 1, ..., N$ and $j = 1, ..., N$). The operation of a threshold device is defined as follows: If the input $x_{ij}(t)$ is below the threshold b, there will be no output $s_{ij}(t)$. If the input increases above threshold, the device responds with a δ spike of intensity i_0, i.e., $s_{ij}(t) = i_0 \Theta(\dot{x}_{ij}) \delta(x_{ij}(t) - b)$. After such a firing event, the device enters a refractory period Δt_r, where it is inactive and not susceptible to any external inputs. We further take into account an exponential leakage of the input due to the interaction with a thermal environment. This is described by the linear Langevin equation for the inputs $x_{ij}(t)$ of the threshold devices

$$\dot{x}_{ij} = -\gamma x_{ij} + \sqrt{\gamma \sigma}\, \xi_{ij}(t), \tag{1}$$

with

$$\langle \xi_{ij}(t) \xi_{mn}(t') \rangle = 2\delta(t - t') \delta_{(im)} \delta_{(jn)},$$
$$\langle \xi_{ij}(t) \rangle = 0,$$
$$\sigma = \langle x_{ij}(t)^2 \rangle, \tag{2}$$

and the leakage constant γ. The Langevin equation (1) can be integrated exactly over the interval Δt, yielding the map [12]

$$x_{ij}(t + \Delta t) = x_{ij}(t) \exp(-\gamma \Delta t) + G, \tag{3}$$

with G being a Gaussian random number with the variance $\sigma_G = \sigma[1 - \exp(-2\gamma \Delta t)]$. The time delay Δt accounts for nonpropagative delay effects between the formation of a pulse and its interaction with another element. In neuronal systems, this time delay describes, e.g., synaptic transmission delays. Introducing dimensionless variables $x \rightarrow x/b, t \rightarrow \gamma t, \bar{\sigma} = \sigma/b^2$ and normalizing the time step unity, we observe that we can describe the threshold device with two parameters, the normalized dissipation $\bar{\gamma} = \gamma \Delta t$ and the normalized variance of the noise $\bar{\sigma}$.

The threshold devices are pulse coupled, i.e., the coupling between them takes place when one of them, say, d_{kl}, fires. It then communicates with its surrounding elements d_{ij}, located at a Euclidean distance $r_{ij,kl}$, by adding

 0031-9007/95/74(11)/2130(4)$06.00

the amount $K\exp(-\lambda r_{ij,kl}^2/a^2)$ to their inputs $x_{ij}(t)$, with $K \to K/b$ in dimensionless units. The dimensionless quantity λ describes the spatial coupling range of the devices. The transfer from all elements d_{kl} spiking at time t to the input of the element d_{ij} at the delayed time (finite traversal time for communication) $t + \Delta t$ is given by

$$\Delta x_{ij}(t + \Delta t) = K \sum_{kl} \exp\left(-\lambda \frac{r_{ij,kl}^2}{a^2}\right). \quad (4)$$

After each time step we carry through a complete update of the array, i.e., we identify elements which are over threshold, reset them, and label them refractory. As boundary conditions for the square lattice we use free boundaries, i.e., excitation can propagate out of the lattice, but no activity can propagate from outside in.

For sufficiently large coupling, i.e., $K \geq \exp(\lambda)$, firing elements are a source for excitatory waves, spreading through the array [13,14]. Typical observed wave forms are spiral waves and target waves [1] (target waves are single, nonrepetitive wave fronts). The selection of the respective pattern is achieved by varying the geometry of the initial conditions. The role of fluctuations in the regime $K \geq \exp(\lambda)$ is twofold. First, the propagation of existing waves is disturbed, i.e., the wave fronts are getting fuzzy but are not destroyed. Second, noise can create spontaneously target waves which collide with the existing wave and with each other. The second effect limits the unperturbed growth of the spiral wave to a finite coherence area, which decreases with increasing noise strength. A detailed analysis of the noise dependence of the size of coherent areas in view of Bunimovich's criteria [15] for the onset of spatiotemporal chaos is in preparation [16].

For smaller values of K, firing elements do not necessarily start an excitational wave. For example, for an initially infinitely extended single column of firing elements, the effective thresholds of the elements in the column next to the firing column are given by

$$\begin{aligned} b_1^{\text{eff}} &= 1 - K\exp(-\lambda)S_0 \\ &\equiv 1 - K\exp(-\lambda)\sum_{n=-\infty}^{\infty}\exp(-\lambda n^2) \\ &\approx 1 - K\sqrt{\frac{\pi}{\lambda}}\exp(-\lambda) \quad \text{for } \lambda \to 0. \end{aligned} \quad (5)$$

This equation is obtained by summing up all the contributions of the elements along the firing column to the inputs of the neurons in a neighboring column and then subtracting it from the "undressed" threshold. In order that a wave starts to spread spontaneously, the coupling has to be larger than $K_c(\lambda) = \sqrt{\lambda/\pi}\exp(\lambda)$.

In the presence of noise, however, we observe spreading of excitatory waves also in the subthreshold regime, i.e., for $K < K_c$. In Fig. 1, we have shown snapshots of a noise-sustained rotating spiral wave, grown out of an initial column of firing elements for $K = 0.151 < K_c(\lambda = 0.1) = 0.1971$ (subthreshold) and $\bar{\gamma} = 0.5$. Turning off the noise, the spiral will eventually disappear [see Fig. 1(a)]. The scale of the noise sustained spiral wave

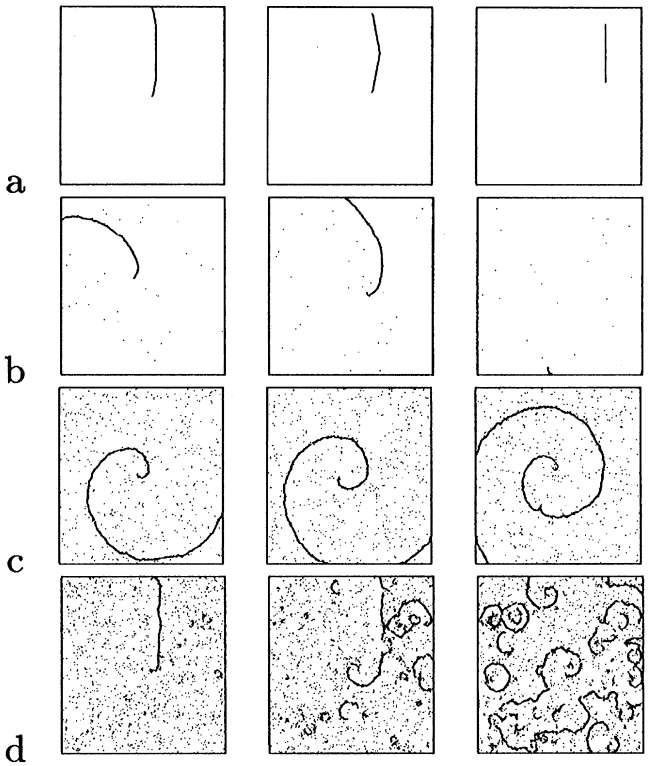

FIG. 1. Formation of a spiral wave in an array of 400 × 400 threshold elements out of an initially firing column of elements for $K = 0.151, \bar{\gamma} = 0.5, \lambda = 0.1$. A layer of refractory elements was attached to the left side of the initially firing column. The frames from left to right represent snapshots of firing patterns of threshold elements at positions (i, j) with $i, j = 1, ..., 400$ as time evolves. The dots denote firing elements. In (a) the noise was turned off, while (b), (c), and (d) correspond to the noise levels $\bar{\sigma} = 0.08, 0.13$, and $\bar{\sigma} = 0.15$, respectively.

is determined by the ratio of the longitudinal (normal to the front of firing elements) and the transversal (parallel to the front) speed of excitatory propagation. For increasing noise, the noise-induced transversal propagation speeds up, yielding a spiral wave with a larger curvature [compare Figs. 1(b) and 1(c)], i.e., a larger degree of coherent activity in the array. On the other hand, if the noise becomes too large, breakup of spirals and spontaneous nucleation of other spirals will destroy the coherent activity [see Fig. 1(d)]. The value for the noise strength $\bar{\sigma}_{\text{opt}}$ at which the coherent activity is optimized can be derived approximately by identifying the effective threshold for the noise-induced growth of a spiral wave. Having a single column of firing elements, the effective threshold for the transversal growth is (for small λ) larger than the effective threshold for exciting an element in the column next to the nearest column of the firing front, i.e.,

$$b_{\text{eff}}^{\text{nn}} \approx 1 - K\exp(-2\lambda)S_0 \approx 1 - K\sqrt{\pi/\lambda}\exp(-2\lambda). \quad (6)$$

Having once established a layer of two firing columns of elements, the effective threshold for transversal growth

is smaller than $b_{\mathrm{eff}}^{\mathrm{nn}}$. Since the largest threshold in a row of two threshold processes determines the relevant time scale of the growth process, $b_{\mathrm{eff}}^{\mathrm{nn}}$ can be identified as the effective threshold for spiral growth in the subthreshold regime. The optimal value for the noise is obtained by using the spiking threshold elements that are most sensitive to external perturbations if the variance of the noise is half of the square of the threshold [9], i.e., $\bar{\sigma}_{\mathrm{opt}} = (1/2)(b_{\mathrm{eff}}^{\mathrm{nn}})^2 \approx 0.009$ (for $\lambda = 0.1$). The arguments above are, of course, very idealized. They neglect inhomogeneities in the effective threshold around the tip of a firing front and memory effects, but give good first order approximations.

In the main part of this paper, we want to show that the above found effect of noise induced spatiotemporal coherence is actually spatiotemporal stochastic resonance (STSR). In order to make a connection to the notion of stochastic resonance, we drive our array with a solitary *wave* by modulating the inputs of the threshold devices according to

$$x_{ij}(t) \rightarrow x_{ij}(t) + A\delta_{i_0+nc,i}, \qquad j = 1, 2, \ldots, N, \qquad (7)$$

where c is the speed of propagation. The response of the array is a spatiotemporal pattern of firing activity. We characterize STSR by the time averaged number of excess events (TANEE) η at the position of the wave. TANEE is defined as the difference of the number of firing elements along the front of the driving wave (a row of the array) and the average number of firing events along a row of the array, not affected by the driving. This number is averaged over about 10 000 time steps to yield the time averaged number of excess events. In Fig. 2, we show three snapshots of firing pattern, obtained by operating an array of 200 × 200 elements at different values of the noise level and $K = 0.121$ ($K_c = 0.1971$). For the smallest noise strength, we can hardly see any impact of the driving wave on the firing pattern, i.e., an increase of firing activity along the driving wave. Accordingly, TANEE is relatively small [see Fig. 3(a)]. Increasing the noise strength, we observe the formation of clusters of activity, spatially synchronized with the driving wave. The time averaged number of excess events, correspondingly, strongly increases. A snapshot of the firing pattern at the value of the noise strength where we observe a maximum of TANEE [see Fig. 3(a)] is shown in Fig. 2(b). For a further increasing noise level, firing events uncorrelated with the driving wave start to dominate the array and we observe a decay of TANEE. The observed synchronization of the spatiotemporal firing pattern to an externally applied pattern is the canonical generalization of stochastic resonance in ordinary dynamical processes. The time averaged number of excess events η scales linear with the system size (number N of rows of the array). This is shown in Fig. 3(b), where we have plotted TANEE, normalized by the system size for $K = 0.121$ and different sizes of the array ($N = 100, 200, 400$). Apart from a weak system-size dependence around the peak, the curves show universality with respect to system size. It is also remarkable that the maximum of TANEE shows a nonmonotonous dependence on the coupling strength. A similar phenomenon has been observed for the response of a globally coupled array of bistable elements to periodic forcing [17].

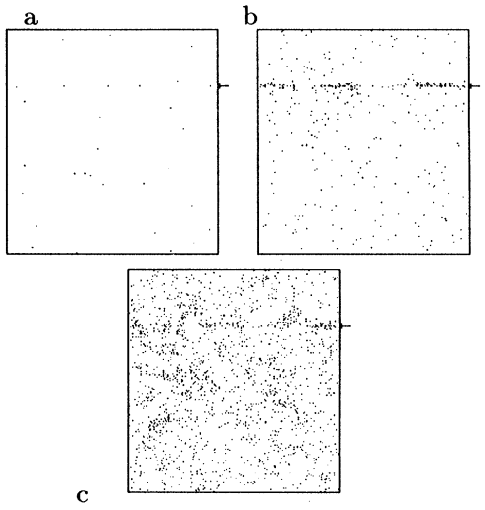

FIG. 2. Snapshots of the firing patterns of an 200 × 200 array ($K = 0.121, \lambda = 0.1, \gamma = 0.5, A = 0.3$) are shown for $\bar{\sigma} = 0.1$ (a), $\bar{\sigma} = 0.16$ (b), and $\bar{\sigma} = 0.2$ (c). The pointers on the right side indicate the position of the driving wave. The dots denote firing elements.

In the zero-coupling limit $K \rightarrow 0$, the optimal noise value $\bar{\sigma}_0^u = 0.5$ is obtained by assuming independent threshold elements [see Fig. 3(a)]. For strong coupling, i.e., when the cluster size of firing elements becomes larger than $1/\lambda$, we approximately assume that a complete line of elements is firing. Subtracting all their contributions to the thresholds of the elements next to the line, we obtain the effective threshold b_1^{eff} [see Eq. (5)]. The optimal noise value for the strong-coupling limit $\bar{\sigma}_0^l = (1/2)(b_1^{\mathrm{eff}})^2$ is shifted to smaller values of the noise strength in comparison to the zero-coupling limit. This finding is

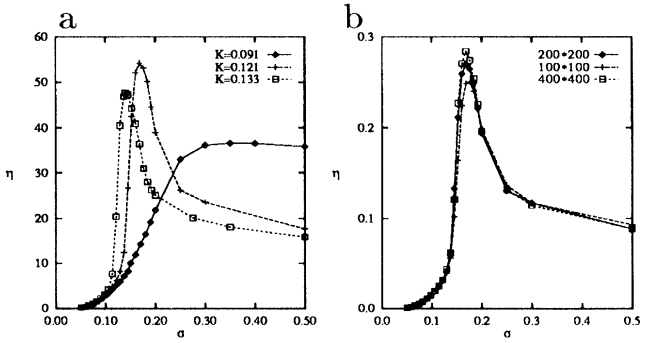

FIG. 3. The TANEE is shown in (a) for three values of the coupling K as a function of the variance of the noise for $\lambda = 0.1, \bar{\gamma} = 0.5$ and $A = 0.3$. The sizes of the symbols represent the accuracy of the data points. In (b), TANEE, normalized by the system size N, is shown for the same set of parameters as in (a) at $K = 0.121$ and different sizes of the array ($N = 100$, $N = 200$, $N = 400$).

confirmed by the results of our computer simulations in Fig. 3(a). It is important to note that the discussion above applies only if we operate our array under subthreshold conditions, i.e., $A < b_1^{\text{eff}}$.

In the absence of noise, only a totally quiescent phase is stable, i.e., whatever the initial configuration of out network is, it will eventually evolve into a state where all elements are quiescent. Driving the system harder, in order that $1 > A > b_1^{\text{eff}}$, the stable, totally quiescent state coexists with a state where all elements fire perfectly synchronized with the driving wave. Noise will induce transition between both stable states. For $A > 1$, the totally quiescent state becomes unstable and we have only the perfectly synchronized state as a stable state. A detailed analysis of this spatiotemporal bistability will be presented elsewhere [16].

In conclusion, this is the first report of spatiotemporal stochastic resonance in a two-dimensional excitable medium. Driving the array by a solitary wave, we found that the synchronization of the firing pattern to the driving shows a resonance peak as a function of the noise strength—the fingerprint of stochastic resonance. We further have pointed out a direct application, namely the spatiotemporal, parametric control of spiral waves. The size of the coherent domains in the array (i.e., the size of a domain where one spiral lives) can be controlled very sensitively by the noise level. These results might open new ways of understanding the spatiotemporal dynamics in neuronal systems, such as the origination of epileptic seizures [14]—especially the up to now unexplored function of noise. It might also suggest new ways of controlling spatiotemporal structures in the atmosphere.

P. J. wishes to thank the Deutsche Forschungsgemeinschaft for financial support. We also would like to acknowledge stimulating discussions with Andreas Herz, L. A. Bunimovich, J. Cowan, J. Milton, and A. Hubler.

[1] M. C. Cross and P. C. Hohenberg, Rev. Mod. Phys. **65**, 851 (1993).
[2] A. T. Winfree, Chaos **1**, 303 (1991).
[3] J. Stat. Phys., edited by H. R. Brand, C. R. Doering, and R. E. Ecke **54**, 1111 (1989).
[4] P. C. Hohenberg and J. B. Swift, Phys. Rev. A **46**, 4773 (1992).
[5] *Noise in Dynamical Systems,* edited by F. Moss and P. V. E. McClintock (Cambridge University Press, Cambridge, U.K., 1989), Vol. i-iii.
[6] R. Benzi, A. Sutera, and A. Vulpiani, J. Phys. A **14**, l453 (1981); B. McNamara and K. Wiesenfeld, Phys. Rev. A **39**, 4854 (1989); B. McNamara, K. Wiesenfeld, and R. Roy, Phys. Rev. Lett. **60**, 2626 (1988); L. Gammaitoni, F. Marchesoni, E. Manichella-Saetta, and S. Santucci, *ibid.* **62**, 349 (1989); P. Jung and P. Hanggi, Europhys. Lett. **8**, 505 (1989); Hu Gang, G. Nicolis, and C. Nicolis, Phys. Rev. A **42**, 2030 (1990); M. I. Dykman, R. Mannella, P. V. E. McClintock, and N. G. Stocks, Phys. Rev. Lett. **65**, 2606 (1990); P. Jung and P. Hanggi, Phys. Rev. A **44**, 8032 (1991); J. Stat. Phys., edited by F. Moss, A. Bulsara, and M. Shlesinger **70**, 1–514 (1993); R. F. Fox and Yan-nan Lu, Phys. Rev. E **48**, 3390 (1993); John K. Douglas, Lon Wilkens, Eleni Pentazelou, and Frank Moss, Nature (London) **365** (1993).
[7] P. Jung, Phys. Rep. **234**, 175 (1993).
[8] F. Moss, in *Frontiers in Applied Mathematics,* edited by G. Weiss (SIAM, Philadelphia, 1992).
[9] P. Jung and G. Mayer-Kress, Nuovo Cimento (to be published).
[10] P. Jung, Phys. Rev. E **50**, 2513 (1994).
[11] Z. Gingl, L. Kiss, and F. Moss, Europhys. Lett. **29**, 191 (1995).
[12] R. F. Fox, Phys. Rev. A **43**, 2649 (1991).
[13] P. Jung and G. Mayer-Kress (to be published).
[14] J. G. Milton, P. H. Chu, and J. D. Cowan, in *Advances in Neural Information Processing,* edited by S. J. Hanson, J. D. Cowan, and C. L. Giles (Morgan Kaufman, San Mateo, CA, 1993), Vol. 5, p. 1001; P. H. Chu, J. G. Milton, and J. D. Cowan, Int. J. Bif. Chaos **4**, 237 (1994).
[15] V. S. Afraimovich and L. A. Bunimovich, Physica (Amsterdam) (to be published).
[16] P. Jung and G. Mayer-Kress (to be published).
[17] P. Jung, U. Behn, E. Pentazelou, and F. Moss, Phys. Rev. A **46**, R1709 (1992).